H. CATTANEO ✉
T. LAURILA
R. HERNBERG

Photoacoustic detection of oxygen using cantilever enhanced technique

Tampere University of Technology, Institute of Physics, Optics Laboratory,
P.O. Box 692, 33101 Tampere, Finland

ABSTRACT A tunable diode laser photoacoustic setup based on a recently demonstrated cantilever technique was used for sensitive detection of oxygen. As light sources, we used a distributed feedback (DFB) diode laser and a vertical-cavity surface-emitting (VCSEL) laser, both operating near 760 nm. With the 30 mW DFB laser a noise-equivalent detection limit of 20 ppm for oxygen was obtained, while a detection limit of 5‰ was achieved with the VCSEL having an output power of 0.5 mW. Our results yield a noise-equivalent sensitivity of 4.8×10^{-9} $cm^{-1} W Hz^{-1/2}$ and demonstrate the potential of this technique for compact and sensitive measurement of oxygen.

PACS 42.62.Fi; 42.55.Px; 82.80.Kq

1 Introduction

Sensitive detection of oxygen is essential in many industrial and research applications. These include medical, biological, and physiological applications (e.g., breath diagnostics, studies on metabolism and fermentation, and monitoring of sport activities), energy management and production control (e.g., gas purity in semiconductor industry, food storage, and power generation in combustion), as well as environmental monitoring. These applications necessitate detection limits ranging from sub-ppm levels at low pressures to several per cents at atmospheric conditions. Due to such diverse requirements, various types of oxygen sensors have been developed, which are based on the electrochemical and physical properties of oxygen. Examples of commonly exploited technologies include electro-chemical cells [1], ion conductivity of ceramics (mostly ZrO_2) [2], paramagnetism [3], adsorption on semiconducting metal oxides [4], and fluorescence quenching [5].

Many of the applications listed above would benefit from a sensitive, small, portable, stable, non-intrusive, and possibly cheap oxygen sensor. All-optical oxygen sensors based on absorption spectroscopy and near-infrared diode lasers have the

✉ Fax: +358 3 31152090, E-mail: heidi.cattaneo@tut.fi

potential of meeting most of these stringent requirements and have been exploited widely in industrial applications [6–11]. Vertical-cavity surface-emitting lasers (VCSELs) are favored for tunable diode laser spectroscopy (TDLS) of oxygen because of their advantages over traditional diode lasers, such as single-mode operation, good beam quality, high repetition rate, relatively narrow line width, large current tuning range, good operability, and low power consumption. Moreover, VCSELs have the potential of being low-cost devices due to their moderate fabrication costs.

Unfortunately, small size is hardly achieved with oxygen sensors based on TDLS. This is due to the fact that the only absorption band of oxygen within the spectral range covered by diode lasers is a weak magnetic dipole transition around 760 nm. As the minimum detectable optical density with TDSL is typically on the order of 10^{-4} and the line strengths of oxygen transitions are on the order of 10^{-24} $cm^2/(cm$ molec), an absorption path length of several tens of cm is needed to detect 1% oxygen levels at atmospheric conditions. The path length can be reduced by using wavelength modulation or balanced detection [11], which improve the sensitivity of TDLS sensors. Although the detection of optical densities on the order of 10^{-6}–10^{-7} has been demonstrated [11], such sensitivities are difficult to obtain in field measurements.

Photoacoustic spectroscopy (PAS) is a well-known technique for sensitive gas analysis. Recently, it has been combined with tunable diode lasers, allowing optical densities of $\sim 10^{-7}$ to be detected [12, 13]. Due to the relatively high sensitivity, PAS can potentially yield smaller sensors compared to traditional absorption methods [14]. However, PAS is a power scalable technique and therefore calls for excitation sources with high output powers. As the power levels of VCSELs are typically below 1 mW, conventional PAS arrangements would only permit the measurement of relatively high optical densities with VCSEL based excitation. Therefore TDLPAS applications usually utilize distributed feedback (DFB) lasers, which typically provide more than 30 mW output power. Recently, we demonstrated a novel and sensitive TDLPAS setup [15, 16], which is based on cantilever-enhanced detection [17]. A normalized sensitivity of 2.2×10^{-9} $cm^{-1} W Hz^{-1/2}$ for CO_2 detection at 1572 nm

was achieved [18, 19]. Such a high sensitivity suggests that reasonable detection limits for oxygen could also be achieved using low power light sources such as VCSELs.

In this work, a compact photoacoustic setup utilizing interferometrically-enhanced cantilever-based detection has been used for oxygen sensing near 760 nm. A DFB laser and a VCSEL were used as light sources. The lasers had an output power of 30 mW and 0.5 mW, respectively. A noise-equivalent detection limit of 20 ppm was obtained with the DFB laser, whereas the VCSEL measurements yielded a detection limit of 5‰. With the used DFB setup, our results yielded a noise equivalent sensitivity of 4.8×10^{-9} cm^{-1}W Hz$^{-1/2}$. The stability of the system was investigated by measuring the Allan variance of the detected signals.

2   Experimental

The light sources used in our experiment were a DFB laser from Toptica Photonics (LD-0763-0050-DFB-1) operating at 763 nm and a VCSEL from Avalon Photonics (Laser Components, Specidilas V-763-OXY-MTE) operating at 762 nm, both having an integrated TEC element. The side mode suppression ratios were 40 dB and 30 dB, respectively. The maximum output power levels in single mode were 50 mW and 0.5 mW. The beam profile of the DFB laser was elliptical with beam divergences of 8° and 2° whereas the VCSEL had a circular beam profile and a 12° beam divergence. Due to the circular beam profile, the light beam from the VCSEL was more efficiently coupled through the 3 mm diameter photoacoustic cell than the beam of the DFB laser.

A temperature controller (ILX Lightwave LDT-5525) and current controllers (ILX Lightwave LDX-3220 for the DFB laser and LDX-3210 for the VCSEL) were used to adjust the operation temperature and injection current of the lasers. The linear current tuning coefficients were 0.0025 nm/mA for the DFB laser and 0.26 nm/mA for the VCSEL. Although the current tuning coefficient of the VCSEL was two orders of magnitude larger than that of the DFB laser, single-mode operation of the VCSEL was maintained for a smaller current range. The lateral multimode regime of the VCSEL started at a current of $1.8 I_{th}$, where I_{th} is the current threshold, resulting in a 0.5 nm single mode current tuning range. The DFB laser was operated in single mode throughout the whole operation regime. The useful tuning ranges for the two lasers were therefore comparable. The temperature tuning coefficients were 0.052 nm/K (DFB) and 0.057 nm/K (VCSEL). The temperature and the DC bias current of the lasers were first tuned to drive the laser wavelength close to the desired absorption feature. The modulation required for PAS was obtained by sinusoidally modulating the laser current (Agilent 33250A signal generator) to scan the laser wavelength across the absorption feature.

Oxygen has a weak magnetic-dipole-allowed absorption band near 760 nm. Part of the P-branch around 763 nm could be reached with the diode lasers used. The targeted absorption lines were simulated with the HITRAN database [20] and are shown in Fig. 1. The simulation assumed a path length of 6 cm, a total pressure of 250 mbar and an oxygen concentration of 500 ppm. As can be seen in the
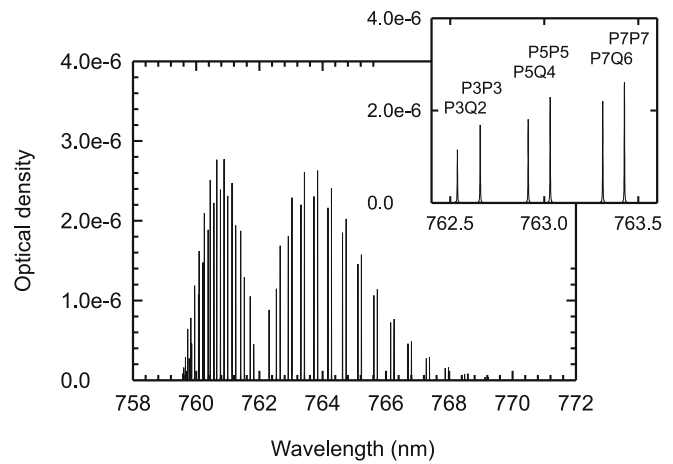

FIGURE 1   Absorption spectrum of oxygen in the 760 nm region, simulated by assuming a path length of 6 cm, a total pressure of 250 mbar, and an oxygen mole fraction of 500 ppm. The *inset* shows the investigated lines (*P*3*Q*2 and *P*7*P*7)

figure, the optical density levels are small and difficult to measure with direct absorption methods. The investigated absorption lines were the *P*7*P*7 line at 763.43 nm (DFB) and the *P*3*Q*2 line at 762.54 nm (VCSEL). The line strengths of these lines are 8.48×10^{-24} cm^2/(cm molec) and 3.91×10^{-24} cm^2/(cm molec), respectively.

The experimental setup is shown in Fig. 2. The modulated laser beam was coupled through a small photoacoustic cell (diameter 3 mm, length 6.1 cm), using an aspheric collimating lens. The volume of the cell including small buffer volumes was 1.7 cm^3. The volume behind the cantilever was 17 cm^3. The laser beam was incident at the Brewster angle on the fused silica windows of the photoacoustic cell and the polarization was matched by using a zero-order half-wave plate or rotating the laser. The transmitted power was monitored with a power meter. The induced photoacoustic signals were detected using a micro-mechanical cantilever transducer having dimensions of 6 mm × 2 mm × 10 μm (length, width, and thickness). The gap between the cantilever and the frame was 3 μm. A compact optical Michelson interferometer was used to monitor the deflections of the cantilever. The fringe pattern of the interferometer was recorded using three photodiodes and a Fourier transform (FFT) was calculated from the amplified and preprocessed photodiode signals. The data acquisition was synchronized to the laser modulation and the FFT spectrum was obtained by averaging 100 individual data acquisitions, leading to a measurement time of 68 s. More de-
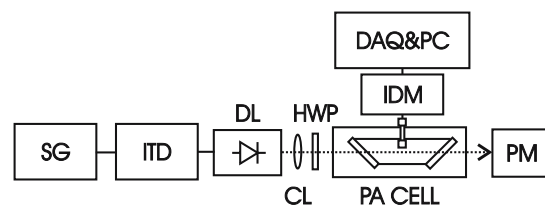

FIGURE 2   Experimental setup. SG–signal generator; ITD–current and temperature driver; DL–diode laser; CL–collimation lens; HWP–half-wave plate; PA CELL–photoacoustic cell; IDM–interferometric detection module; DAQ&PC–16-bit data acquisition board and personal computer; PM–power meter

tailed explanation of the detection method can be found in earlier publications [15, 16, 18, 19].

3   Results and discussion

The photoacoustic signal depends on the gas pressure, modulation amplitude and modulation frequency. A total gas pressure of 250 mbar was used. Several measurement series were made to determine the optimum modulation amplitude and frequency. The dependence of the signal amplitude, noise levels, and signal to noise ratio on the modulation frequency using DFB laser is shown in Fig. 3. During the measurements the modulation amplitude was 70 mV_{pp}, and the O_2 concentration was 5000 ppm. The signal amplitudes were obtained by subtracting the background levels from the peak values at the detection frequency of $2f_{mod}$. The noise levels were determined as the standard deviation over the 50 Hz bandwidth around $2f_{mod}$. As can be seen in the figure, the optimum modulation frequency was close to 40 Hz.

The optimum modulation amplitude was determined separately for the DFB laser and for the VCSEL (Fig. 4). The obtained amplitude values of 70 mV_{pp} (DFB) and 3.0 mV_{pp} (VCSEL) differ from each other due to the different current tuning coefficient of the lasers and different tuning characteristics of the current drivers. When expressed in wavelength units, however, these values correspond to modulation amplitudes of 7.3 pm and 7.2 pm, respectively. During the modulation amplitude optimization the O_2 concentrations were 1000 ppm and 25% when using the DFB laser and the VCSEL, respectively. Under these conditions the absorption linewidths are 2.6 pm (1000 ppm of O_2 in N_2 at 763.43 nm) and 2.7 pm (25% of O_2 in N_2 at 762.54 nm) yielding modulation indices ($m = \Delta\nu_{mod}/\Delta\nu_{line}$) of 2.8 and 2.7, respectively.

The photoacoustic signal as a function of the O_2 concentration is shown in Fig. 5 for the two lasers. In these measurements, the desired oxygen concentrations were obtained by diluting pure oxygen or O_2/N_2 pre-mixtures of different concentrations (10%, 2.5%, 5000 ppm, and 1000 ppm) in pure nitrogen by using mass flow controllers. The measurements were performed with the DFB laser operating at 30 mW and
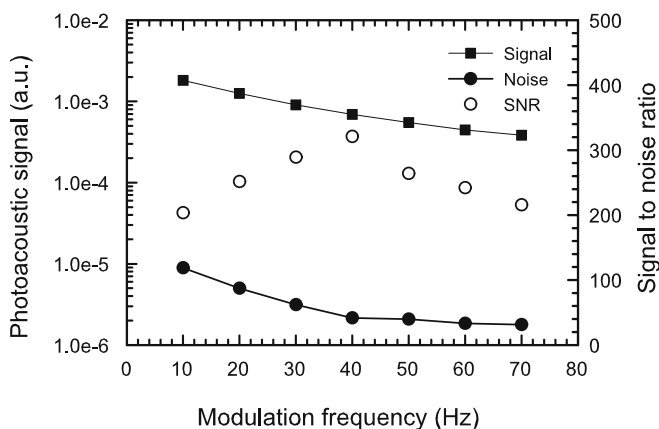

FIGURE 4   System's response to modulation amplitude. The measurements were performed with a gas pressure of 250 mbar, a modulation frequency of 40 Hz, and an oxygen concentration of 1000 ppm for the DFB laser and of 25% for the VCSEL

the VCSEL operating at 0.5 mW. As can be seen from the figure, the DFB laser yields a much better detection limit due to its higher output power. A linear fit to the data gives a noise-equivalent (1σ) detection limit of 20 ppm for the DFB laser. From these results, and taking into account the lower output power of the VCSEL and the lower line strength of the $P3Q2$ absorption line, the detection limit for the VCSEL was estimated to be 3 ‰. Our measurements with the VCSEL yielded a detection limit of 5 ‰ for oxygen. This small difference may be due to the fact that the cantilever was damaged after the DFB measurements and had to be replaced by a new one.

We note that the detection method employed in this study is integrative and not purely spectral as in other TDLPAS

FIGURE 3   System's response to modulation frequency. Signal and background levels are measured at $2f_{mod}$ and noise level is the standard deviation over the 50 Hz bandwidth around the detection frequency. The measurements were performed at a pressure of 250 mbar, an oxygen concentration of 5000 ppm, and a modulation amplitude of 70 mV_{pp}
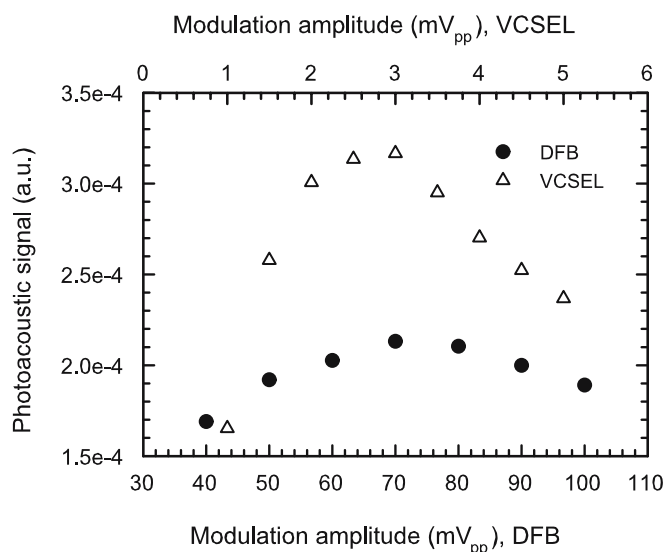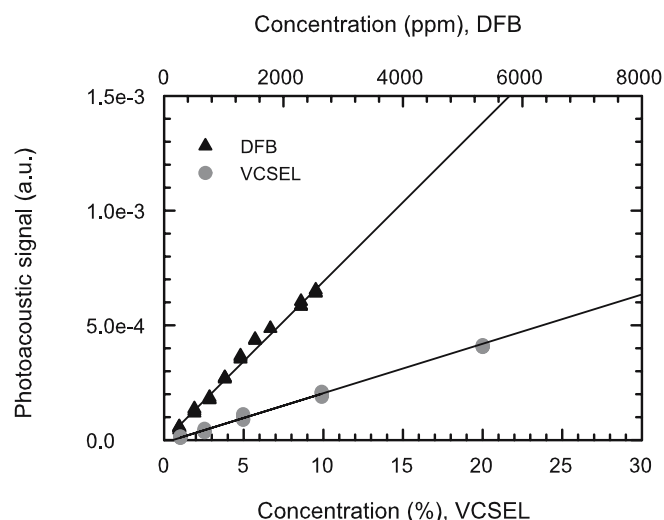

FIGURE 5   Photoacoustic signals obtained as a function of the O_2 concentration. The measurements were performed with a gas pressure of 290 mbar and a modulation amplitude of 70 mV_{pp} (for the DFB laser), and 250 mbar and 3 mV_{pp} (for the VCSEL). The modulation frequency was 40 Hz. The power levels in the measurements were 30 mW and 0.5 mW for the DFB laser and for the VCSEL, respectively

arrangements. Spectral sensitivity values as determined for example in references [14] and [21] are therefore not directly obtainable in our case. With the measurement parameters used with the DFB laser, a noise equivalent sensitivity of $4.8 \times 10^{-9}\,\mathrm{cm^{-1}W\,Hz^{-1/2}}$ was calculated. The sensitivity is normalized with respect to power and measurement bandwidth and assumes a Voigt absorption profile. The sensitivity is comparable to the values reported by other groups employing tunable diode lasers [14, 21]. The calculated sensitivity value is slightly poorer than that obtained in previous measurements with CO_2 (in Ar) [18, 19]. The values for minimum detectable absorption coefficient ($\alpha_{\min}$) and optical density ($\alpha_{\min}l$) are $1.9 \times 10^{-8}\,\mathrm{cm^{-1}}$ and 1.1×10^{-7}, respectively. These results fall short of sensitivity levels ultimately achievable and earlier demonstrated with highly optimized systems and powerful lasers. Nevertheless, the results show that the presented technique can be utilized for small-size oxygen sensors of high sensitivity. For practical demands in oxygen sensors, for example in biomedicine, the demonstrated sensitivity is sufficient.

In spectroscopic measurements, the stability of the system is an important issue. One way to characterize the stability is to measure the Allan variance of the signal [22], which was originally introduced for determining frequency stability but can also be used for spectroscopic instruments [23]. The Allan variance can be defined as:

$$\sigma(\tau) = \sqrt{\frac{1}{2(N-1)} \sum_{i=1}^{N-1} \left(\bar{y}_i - \bar{y}_{i+1}\right)^2},$$

where τ is the integration time, N the number of ensemble groups and $\bar{y}_i$ the average of the ensemble group. The stability test of our setup was made with the DFB laser at an oxygen concentration of 5000 ppm. A peak value at $2f_{\mathrm{mod}}$ (80 Hz) of the FTT spectrum was used as an input sample. The data were collected for a period of one hour and N was chosen to be 10. As can be seen in Fig. 6, the Allan variance shows a $\sim 1/\sqrt{\tau}$ dependence, indicating a white noise behavior [23]. The detection limit could, therefore, be slightly improved with a longer integration time. During the one-hou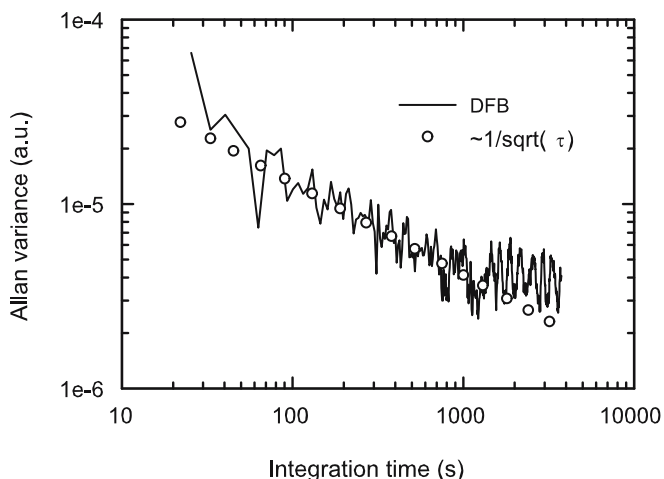r period of the Allan variance measurement the emission wavelength of the DFB laser was stable. We observed that during the one-hour period the VCSEL used to drift slightly (0.8 pm) and therefore would need active stabilization for longer integration times.

The performance of the detection system is influenced by various noise sources. Measurements of Kauppinen et al. [24] on a similar setup indicated that the dominant noise source present in cantilever enhanced photoacoustic arrangements is the ambient acoustic noise. Lowering the pressure reduces the influence of the acoustic noise but also tends to decrease the signal amplitude. At low pressures the limiting noise source is thermal noise. Compared to acoustic and thermal noises, the electric noise of the system is vanishingly small. Also the intensity noise of the excitation laser is negligible compared to the acoustic noise at 250 mbar.

In conclusion, a compact cantilever-enhanced photoacoustic method was demonstrated for sensitive oxygen detection. Two light sources, a 30 mW DFB laser and a 0.5 mW VCSEL, both emitting near 760 nm, were investigated. Our results show that ppm oxygen levels can be detected with this method using a DFB laser as the light source. Detection limits on the order of per mille were also achieved with the VCSEL. The noise equivalent sensitivity of our setup was calculated to be $4.8 \times 10^{-9}\,\mathrm{cm^{-1}W\,Hz^{-1/2}}$. These results demonstrate that small oxygen sensors having absorption lengths in the mm range could be used to measure per mille levels of oxygen when DFB lasers are employed.

REFERENCES

1 R. Kocache, J. Phys. E Sci. Instrum. **19**, 401 (1986)
2 R.M.A. Kocache, J. Swan, D.F. Holman, J. Phys. E Sci. Instrum. **17**, 477 (1984)
3 P.T. Meriläinen, Biomed. Instrum. Technol. **23**, 462 (1989)
4 W.P. Kang, J.F. Xu, B. Lalevic, T.L. Poteat, Sens. Actuators **12**, 349 (1987)
5 J.I. Peterson, R.V. Fitzgerald, Anal. Chem. **56**, 62 (1984)
6 M. Kroll, J.A. McClintock, O. Ollinger, Appl. Phys. Lett. **51**, 1465 (1987)
7 V. Weldon, J. O'Gorman, J.J. Pérez-Camacho, D. McDonald, J. Hegarty, J.C. Conolly, N.A. Morris, J.H. Abeles, Infrared Phys. Technol. **38**, 3259 (1997)
8 I. Linnerud, P. Kaspersen, T. Jæger, Appl. Phys. B **67**, 297 (1998)
9 H.P. Zappe, M. Hess, M. Moser, R. Hövel, K. Gulden, H.-P. Gauggel, F. Monti di Sopra, Appl. Opt. **39**, 2475 (2000)
10 J. Wang, S.T. Sanders, J.B. Jeffries, R.K. Hanson, Appl. Opt. **72**, 865 (2001)
11 P. Vogel, V. Ebert, Appl. Phys. B **72**, 127 (2001)
12 A. Schmohl, A. Miklós, P. Hess, Appl. Opt. **41**, 1819 (2002)
13 A. Miklós, M. Fehér, Infrared Phys. Technol. **37**, 21 (1996)
14 A.A. Kosterev, F.K. Tittel, D.V. Serebryakov, A.L. Malinovsky, I.V. Morozov, Rev. Sci. Instrum. **76**, 043 105 (2005)
15 T. Laurila, H. Cattaneo, V. Koskinen, J. Kauppinen, R. Hernberg, Opt. Express **13**, 2453 (2005)
16 T. Laurila, H. Cattaneo, V. Koskinen, J. Kauppinen, R. Hernberg, Opt. Express **14**, 4195 (2006) Erratum
17 K. Wilcken, J. Kauppinen, Appl. Spectrosc. **57**, 1087 (2003)
18 T. Laurila, H. Cattaneo, T. Pöyhönen, V. Koskinen, J. Kauppinen, R. Hernberg, Appl. Phys. B **83**, 285 (2006)
19 T. Laurila, H. Cattaneo, T. Pöyhönen, V. Koskinen, J. Kauppinen, R. Hernberg, Appl. Phys. B **83**, 669 (2006)
20 L.S. Rothman, D. Jacquemart, A. Barbe, D. Chris Benner, M. Birk, L.R. Brown, M.R. Carleer, C. Chackerian Jr., K. Chance, L.H. Cou-

FIGURE 6 Allan variance as a function of integration time. Measurements were made at concentration of 5000 ppm of O_2 using the DFB laser

dert, V. Dana, V.M. Devi, J.-M. Flaud, R.R. Gamache, A. Goldman, J.-M. Hartmann, K.W. Jucks, A.G. Maki, J.-Y. Mandin, S.T. Massie, J. Orphal, A. Perrin, C.P. Rinsland, M.A.H. Smith, J. Tennyson, R.N. Tolchenov, R.A. Toth, J. Vander Auwera, P. Varanasi, G. Wagner, J. Quantum Spectrosc. Radiat. Transf. **96**, 139 (2005)

21 M.E. Webber, M. Pushkarsky, C.K.N. Patel, Appl. Opt. **42**, 2110 (2005)
22 D.W. Allan, Proc. IEEE **54**, 221 (1966)
23 P. Werle, R. Miicke, F. Slemr, Appl. Phys. B **57**, 131 (1993)
24 J. Kauppinen, V. Koskinen, J. Uotila, I. Kauppinen, Proc. SPIE **5617**, 115 (2004)